Optical Materials 122 (2021) 111702

Contents lists available at ScienceDirect

Optical Materials

journal homepage: www.elsevier.com/locate/optmat

# Plasmon-induced spectral tunability of Perovskite nanowires

Belkıs Gökbulut [a,*], Gokhan Topcu [b], Mustafa M. Demir [b], M. Naci Inci [a]

[a] Department of Physics, Bogazici University, Bebek, 34342, Istanbul, Turkey
[b] Department of Materials Science and Engineering, Izmir Institute of Technology, Urla, 35430, Izmir, Turkey

ARTICLE INFO

*Keywords:*
Gold
Nanocluster
Perovskite
Plasmonics
Spectral-shift

ABSTRACT

In this paper, plasmon-assisted spectral tunability in random media, composed of Perovskite ($CsPbBr_3$) nanowires surrounded by Au nanoparticle clusters in polystyrene matrix, is achieved. The interaction between the surface plasmons and the quantum sources is observed to generate photoluminescence from the higher excited state energy levels of the excited semiconductor nanowires, which results in a blueshifted fluorescence emission of 50 nm. The localized surface plasmon properties are also determined to be tuned by plasmonic pumping of the quantum sources at different resonant frequencies. Thus, the first observation of the tunable blueshifted fluorescence emission of the semiconductor nanocrystals surrounded by plasmonic nanoparticle aggregates is achieved. The dramatic changes in the spectral profiles of the fluorescent nanowires are attributed to be due to the fast dynamics surface enhanced fluorescence mechanism.

## 1. Introduction

Control of the emission dynamics of the quantum light sources, which are close to the metal surfaces, has become an increasingly important technology with the parallel developments in advanced concepts of light-matter interactions [1–3]. Especially, enhanced fluorescence emission dynamics of the light emitters through their interaction with plasmonic nanoparticles, which have an ability to strongly confine the electromagnetic fields within subwavelength regions below the diffraction limit, has attracted a significant research interest with a great potential for designing various light-emitting device applications [4–9]. The strong electromagnetic field induced by a plasmonic nanoparticle, interacting with a fluorophore, results in altered transitions of the fluorophore, which leads to modifications in its emission properties [10]. In recent years, a great deal of efforts has been devoted to explore the interactions between the surface plasmons and the emitting dipoles [11–14]; nonetheless, in most of these studies, the plasmon-induced changes on the spectral profile of the fluorescence emission have not been explored in detail, and only two-level photonic systems have often been asserted [15,16]. However, in real photonic systems, the transitions between different energy levels of the emitter, which is in the close vicinity of the metal nanoparticle, exist in the presence of the localized plasmon resonance to distinctly alter the transition rates, yielding the modified spectral emission profile of the quantum emitter [17]. For instance, using hybrid nanostructures, a plasmon-induced spectral modulation was demonstrated by Zhao et al. [18]. The nanostructure consisted of Au nanorod cores and fluorescent molecules, which were embedded in mesostructured silica shells. A new emission peak of the dye molecules, in addition to the intrinsic one, was observed as the longitudinal plasmon resonance wavelength of the gold nanorod was longer than that of the intrinsic emission peak. The plasmonic resonance frequency was also manifested to be tuned by modifying the distance between two gold nanoparticles, which resulted in dramatic changes in the spectral shape of the fluorescence emission from the dye molecules emitting at the resonators' frequencies through the variations in the spontaneous emission rates [19].

The effects of the surface enhanced fluorescence in both slow and fast dynamics regimes on the variations of the spectral profile of the quantum sources close to the metal surfaces have been investigated, both theoretically and experimentally [20]. When the enhanced decay rate is smaller than the vibrational relaxation rate, slow dynamics surface enhanced fluorescence (SDSEF) induced by the radiative plasmons is observed, which has been researched in a wide range of studies [21–23]. As the total spontaneous emission rate becomes comparable to the internal energy relaxation rate, as a result of the dramatic increase in the radiative decay rate, the fast dynamic surface enhanced fluorescence mechanism (FDSEF) occurs, which causes an obvious blue shift in the wavelength of the fluorescence emission spectrum [24]. Nevertheless, the plasmon-induced blue shift in the fluorescence emission spectrum of the quantum sources has only been reported in a few studies in which

* Corresponding author.
*E-mail address:* belkis.gokbulut@boun.edu.tr (B. Gökbulut).

https://doi.org/10.1016/j.optmat.2021.111702
Received 27 June 2021; Received in revised form 19 September 2021; Accepted 11 October 2021
Available online 19 October 2021

the fluorescence dynamics of the dye molecules close to the metal nanostructures have been unveiled [24]. For instance, hot electroluminescence was generated through a single nanogap between a STP tip and a metal surface, exploring the FDSEF to reveal the electronic dynamics of the molecular fluorescence under the influence of the plasmon resonance of the metal structures [25]. Moreover, excitation laser energy dependent surface enhanced fluorescence from dye molecules on the surface of Ag nanoparticle aggregates was demonstrated to induce a large spectral blueshift of 400 meV, which confirms that the molecular electronic dynamics is dramatically modified in the presence of strong plasmonic fields [26]. Additionally, a tunable blue shift in fluorescence emission spectrum of the dye molecules embedded in a random media composed of Ag nanowires of different aspect ratio was also reported by Bingi et al., which verifies that the spectral modifications are due to the FDSEF [27].

In this work, plasmon-assisted spectral tunability based on random media consisting of Au nanoparticle clusters and Perovskite nanowires (NWs), embedded in a polystyrene (PS) film, is examined for the first time. All-inorganic Perovskites have recently attracted strong research interest due to their outstanding photovoltaic properties [28,29]. In addition, these colloidal semiconductor nanocrystals have been demonstrated to have remarkable intrinsic properties, involving a high photoluminescence yield and stability [30,31]. Especially, in one-dimensional NWs, which are obtained in high aspect ratio, the stability of excitons in quantum wells is enormously enhanced [32]. Furthermore, allowing their dispersion into a variety of solvents and matrices provides them to be utilized in various types of applications such as lasers [33–35] and LEDs [36–38]. In addition to these, Perovskite NWs are highly sensitive to the characteristics of the surrounding environment [39], which significantly affects their fluorescence emission dynamics in the close vicinity of the strong plasmonic field.

In this paper, the random media, composed of Perovskite NWs surrounded by Au nanoparticle clusters in a PS matrix, is excited by a laser beam to exploit the electromagnetic wave-induced collective oscillation of charge carriers on the surface of the plasmonic nanoparticle clusters, generating the dense electromagnetic field regions (hotspots) surrounding the fluorescent NWs. The hot photoluminescence from the higher excited state energy levels of the quantum emitters induces the fast dynamic radiative process, owing to comparable competition with the internal relaxation. The coupling of the excited dipole of the NW into the strong local optical field causes a dramatic spectral blueshift of 50 nm, based on FDSEF mechanism and the localized surface plasmon properties are determined to be modulated by plasmonic pumping of the quantum sources at different resonant frequencies. Thus, the first observation of the tunable blueshifted fluorescence emission of the semiconductor nanocrystals surrounded by plasmonic nanoparticle aggregates is achieved. By this study, the effects of the localized surface plasmons on the spectral modifications of the Perovskite NWs are also elucidated for the first time. Such control of the plasmonic pumping of the quantum sources at different resonant frequencies is demonstrated to be promising, providing a means to effectively tailor the light-matter interaction between the plasmons and the quantum light sources and a new avenue in the design of highly efficient light-emitting device applications such as tunable random lasers made of Perovskite NWs with outstanding photoluminescence characteristics.

## 2. Experimental section

### 2.1. Materials and methods

#### 2.1.1. Synthesis of Au nanoparticles

To obtain stable Au nanoparticles in organic medium, two steps are followed; ionic extraction and reduction. For the former one, Cetyl trimethyl ammonium bromide (CTAB) solution (6.5 mg in 9 mL in chloroform) and $HAuCl_4$ (30 mg in 3 mL water) solution are prepared, respectively. The solutions are mixed and vigorously stirred for 1 h, while color of organic phase changed from colorless into pale yellow. Subsequently, organic phase having CTAB-$Au^{3+}$ complex is separated. For the latter procedure, an amount of $NaBH_4$ (25 mg) is dissolved in water (50 μL) to use as reduction agent. To reduce $Au^{3+}$ ions and obtain spherical particles, fresh reduction agent is carefully added to CTAB-$Au^{3+}$ complex under vigorous stirring. The reduction is conducted until the color of the final solution changed to ruby red.

#### 2.1.2. Synthesis of $CsPbBr_3$ NWs

Cs-oleate, is synthesized by dissolving $Cs_2CO_3$ (0.2 g) and Oleic acid (0.625 mL) in 1-octadecene (7.5 mL). The mixture is loaded to container and dried under vacuum (150 mbar) at 120 °C for 1h. Subsequently, the mixture is heated to 150 °C under $N_2$, and reaction is maintained until all $Cs_2CO_3$ reacted by Oleic acid.

$CsPbBr_3$ NWs are prepared by room temperature crystallization based on the procedure in the literature [40,41]. Initially, Oleic acid (0.125 mL), Oleylamine (0.125 mL), and 1-octadecene (1.25 mL) are loaded into a flask. Thereafter, the 0.1 mL of pre-heated Cs-oleate solution is added to the mixture and the 0.2 mL of $PbBr_2$ precursor solution (0.4 M, heated for 1 h at 80 °C until full dissolution) is finally injected. After 10 s, acetone (5 mL) is rapidly added for crystallization of the $CsPbBr_3$ NWs. Stirring is maintained for 30 min and green precipitates are collected by using centrifuge (6000 rpm, 10 min). The NWs are re-dispersed in toluene with the concentration of 1% w/v.

Before processing with the polystyrene, material properties of Au nanoparticles and $CsPbBr_3$ NWs are investigated in detail. Their characterization results are analyzed and presented in Fig. 1. The Dynamic Light Scattering (DLS) measurement is given in Fig. 1a, which shows that the average size of the Au particles is 13.8 nm, with 0.2 of polydispersity in the form of a single Gaussian distribution. The SEM image of Au nanoparticles given in Fig. 1b confirms the DLS measurement in terms of size and distribution of the nanoparticles, which appear to have spherical shapes. X-ray Diffraction (XRD) analysis is performed to confirm the crystal structure of $CsPbBr_3$, as seen in Fig. 1c. The presented XRD pattern also includes the pattern from the database for a comparison. According to the database JCPDS #54–752, the pattern shows similar characteristics (strong signal at 30.8°) with the orthorhombic crystal structure of $CsPbBr_3$ [42]. The corresponding SEM image of this crystal presented in Fig. 1d reveals that the NWs exist in 1-dimensional shape with a length of about 600 nm and a width of about 20 nm. The emission and extinction spectra of the particles are given in Fig. 1e. The NWs exhibit a sharp emission signal at 483 nm with $\lambda_{exc}$:365 nm source, while it presents two excitation peaks at 340 nm and 425 nm to emit at $\lambda_{em}$:480 nm. On the other hand, the absorption spectrum of the Au nanoparticle dispersion exhibits a peak at 520 nm, being similar to that of the particles with the same size in the literature, which is due to the plasmonic nature of the particles [43,44].

#### 2.1.3. The fabrication of $CsPbBr_3$ NW-Au nanocluster embedded PS films

Au nanoclusters and $CsPbBr_3$ NWs are loaded to polymeric matrix by mixing and drop-casting. The total mixture of $CsPbBr_3$ NWs, Au nanoparticles, and PS solution (30% w/v in THF) are poured onto glass slides to form composite films of various concentrations. A solid content of Au nanoclusters in the films is adjusted from 32 μg to 6.4 μg by diluting the Au nanoparticle solution with chloroform, while $CsPbBr_3$ content is kept constant (Table 1). The mixtures are drop-casted on glass slides and allowed for drying in ambient conditions; afterwards, they are carefully peeled-off.

Au nanoparticles may readily be carried out by integrating them into a polymer matrix [45] in order to make use of their unique electronic properties in a composite structure. Nevertheless, the conventional route for synthesis of Au nanoparticles based on the reduction of $Au^{3+}$ by citrate in water, which has been proposed and improved by Turkevich et al. [46] and Frens [47], limits such integration. Taking the instability of halide perovskites in polar solvents into account, methods for producing stable dispersed Au nanoparticles in nonpolar solvents are

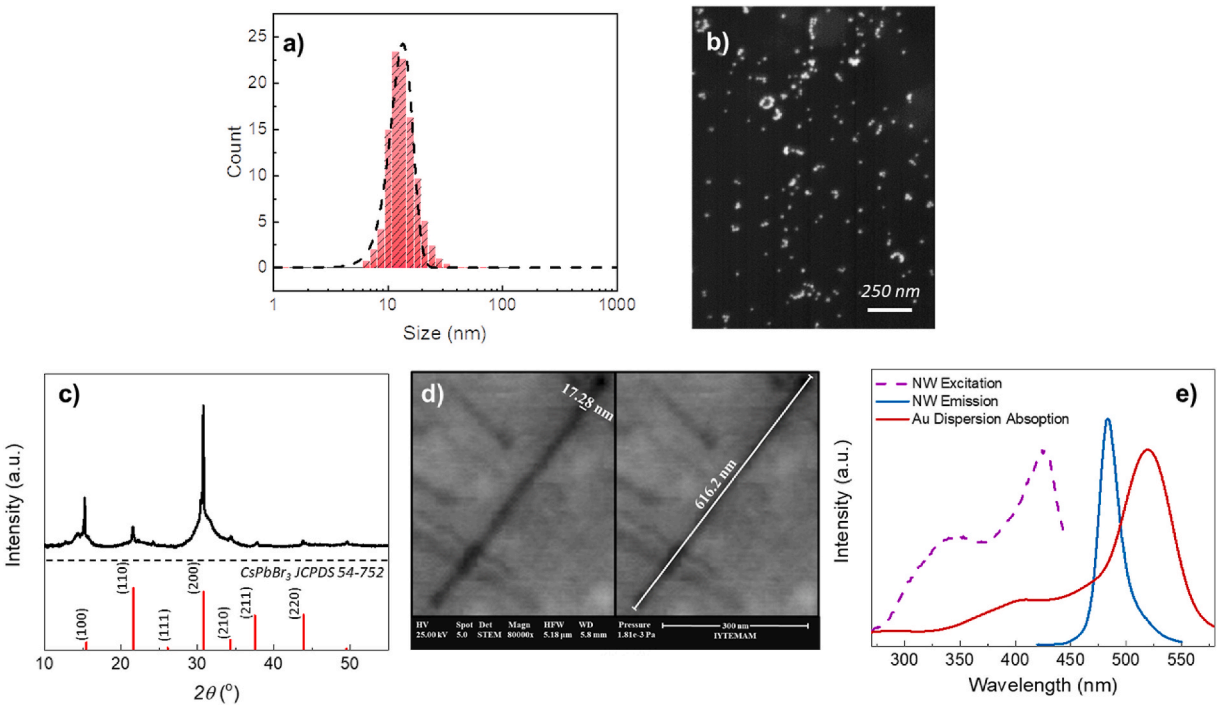


**Fig. 1.** (a) The Dynamic Light Scattering measurement of size and distribution and (b) SEM image of the synthesized Au nanoparticles in a dispersion, (c) X-ray Diffraction pattern and (d) SEM image of $CsPbBr_3$ Perovskite NWs, and (e) PL ($\lambda_{exc}$:365 nm) and PLE ($\lambda_{PL}$:480 nm) spectra of the synthesized $CsPbBr_3$ NWs and absorption spectrum of Au nanoparticles.

**Table 1**
The formula of the prepared films.

| Sample | PS solution *mL* | NW dispersion *mL* | Au NP dispersion *mL* | $CHCl_3$ *mL* |
|---|---|---|---|---|
| **1. Pe/Au40** | 1 | 0.15 | 0.04 | 0.16 |
| **2. Pe/Au66** | 1 | 0.15 | 0.066 | 0.133 |
| **3. Pe/Au100** | 1 | 0.15 | 0.1 | 0.1 |
| **4. Pe/Au200** | 1 | 0.15 | 0.2 | – |

required to compose them in one phase. Due to the need for arduous efforts in direct synthesis of Au nanoparticles in organic solvents, there are only limited studies in the literature compared to alternative methods, involving phase transfer of nanoparticles from aqueous phases into organic one by modifying the nanoparticles using various surfactants [48–52]. In our study, $CsPbBr_3$ NWs are obtained using a simple room temperature anti-solvent crystallization method, while Au nanoparticles are directly synthesized in organic solvent via ion-extraction and integrated into PS matrix.

Table 1 shows the formula of the $CsPbBr_3$ NWs-Au nanoparticle (NP) combined nanostructures, which are embedded in PS films to facilitate altering the emission characteristics of the surrounding quantum sources with their distinctive plasmonic properties.

## 3. Results and discussion

Fig. 2a demonstrates the scanning electron microscopy (SEM) image of the cross-sectional face of a PS film, composed of Perovskite NWs surrounded by Au nanoparticle aggregates, as given in Table 1, by the name of Pe/Au200. The detailed SEM images of the Au nanoparticle aggregates in polystyrene matrix, are also demonstrated in Fig. 2b to elucidate the distinctive morphological characteristics of various plasmonic nanoclusters in the samples.

In our samples, since the fluorescent quantum emitters are confined within the Au nanoparticles and the nanostructures are embedded into the Polystyrene material, the SEM images of the nanostructures, consisting of the Perovskite NWs, surrounded by the aggregated Au nanoparticles, do not explicitly demonstrate the fluorescent NWs, as shown in Fig. 2. It is also significant to emphasize that SEM images in Fig. 2 are taken from a polymer nanocomposite. Since perovskites are semiconductors, they are not clearly distinguishable in the polymer medium because of their lower electron response compared to Au nanoparticles. Therefore, only the Au nanoparticle clusters can be observed in the polymer medium as bright spots because of their conductive nature.

On the excitation of the samples, which consists of Perovskite NWs embedded in Au nanoparticle clusters in PS film with a refractive index ($n_{ps}$) of 1.6, at the wavelength of 405 nm with a laser beam (LDH-D-C-405 Picoquant, GmbH), the strongly localized electromagnetic field signal, induced by the interaction of the surface plasmons with the semiconductor nanocrystals, is collected by an objective lens (Obj. Lens) with a numerical aperture of 0.7, as demonstrated in Fig. 3a. The plasmonic pumping of the dipole of the semiconductor NW, embedded in the metal nanoparticle aggregate, induces the FDSEF mechanism, which results in a blueshifted fluorescence emission signal, as shown in Fig. 3b. The strongly localized field between the plasmonic nanoparticles, manifested by an electric field distribution profile of the dipole of the NW, surrounded by the gold nanoparticle cluster, is also demonstrated in Fig. 3b. The intense local optical field is monitored by a CCD camera (Optronis-1836-ST-153); and then, the emission spectra of the Perovskite NWs enclosed by the Au nanoparticles, are recorded by a photospectrometer (Ocean Optics). Although the thickness of the plasmonic nanoparticle aggregates in PS media varies from 74 nm to 282 nm with distinctive morphological properties, as seen in Fig. 2, the emission spectra from the largest plasmonic nanoparticle clusters surrounding the fluorescent emitters are investigated for each sample with a different Au nanoparticle concentration (see Table 1).

The surface enhanced fluorescence emission spectra of the neat NWs in polymer medium and the NWs embedded in specific Au nanoparticle clusters in a PS thin film are demonstrated in Fig. 4a. The fluorescence emission intensity of the emitting dipoles interacting with the strong

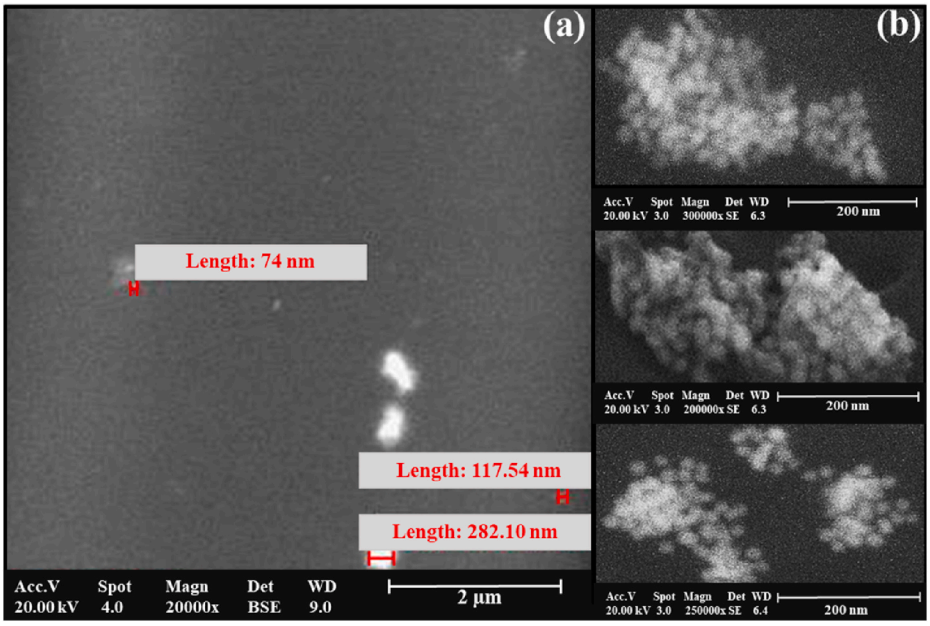


**Fig. 2.** SEM images of (a) the cross-sectional face of a random PS film composed of Perovskite NWs embedded in Au nanoparticle clusters and (b) the gold nanoparticle aggregates in the samples.

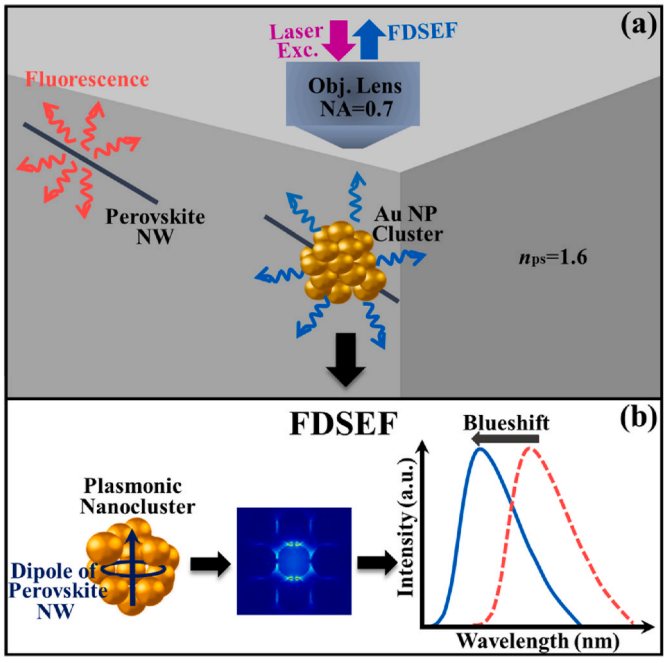


**Fig. 3.** The schematic diagram of a (a) Perovskite NW surrounded by a Au nanoparticle cluster, which is embedded in PS thin film to demonstrate the excitation and collection of the plasmon induced fluorescence signal of the quantum source, and (b) the FDSEF mechanism.

plasmonic field around the Au nanoparticles is observed to be enhanced by about 60% for the sample of Pe/Au40 while it is considerably decreased for that of the samples Pe/Au66, Pe/Au100, and Pe/Au200.

Fig. 4b demonstrates the normalized emission spectra of the semiconductor NWs embedded in a bare polymer medium and specific Au nanoparticle clusters in the random polymer media obtained from the samples given in Table 1. As demonstrated in Fig. 4b, the central emission peak wavelength of Perovskite NWs in polymer material (Pe) is determined to be 526.3 nm. The redshift in the emission of Perovskite NWs in polystyrene compared to Fig. 1e arises from lack of quantum confinement due to forming bundles of Perovskite in polymer [53]. The peak fluorescence emission signals of the nanocrystals surrounded by Au nanoparticle aggregates with different plasmonic characteristics, obtained from the samples of Pe/Au40, Pe/Au66, Pe/Au100, and Pe/Au200, are observed to occur at different emission wavelengths of 510.3 nm, 500.2 nm, 493.0 nm, and 476.6 nm, respectively; which clearly exhibit a significant blueshift in all emission wavelengths compared to that of the semiconductor NWs in the absence of the plasmonic nanoparticle aggregates. The different amount of the blueshift in the fluorescence emission wavelength of the quantum sources, surrounded by specific Au nanoparticle clusters, is induced by a particular plasmon resonance wavelength of each metal nanocluster. This also explicitly reveals the effects of the distinctive higher excited state energy levels of the quantum emitters interacting with the surface plasmons of the specific gold nanoparticle nanoclusters on the spectral emission profiles through the coupling of the excited dipoles of the NWs into the strong local optical fields. Thus and so, control of the plasmon-induced characteristics of the metal nanoparticle clusters in random media allows the tunability of the spectral modulation of the interacting fluorescent nanocrystals.

The blueshift in the fluorescence emission spectrum of the excited NWs interacting with the hotspots is induced by the FDSEF mechanism. Fig. 5 depicts the energy level diagrams and the corresponding electronic transitions from the excited ($S_1$) states to the ground ($S_0$) states for the NWs embedded in a neat polymer and in a hotspot region originating from a random PS medium consisting of Au nanoparticle aggregates to demonstrate the fluorescence and FDSEF mechanisms. For the fluorescent emitters in the polymer medium, the internal relaxation rate from $S_1(\omega_{ex}\text{-}\,\omega_0)$ to $S_1(0)$ is $\Gamma_{int} \approx 10^{12}s^{-1}$, which is much faster than the total decay rate $\Gamma_{tot}$ $(\Gamma_{r0}+\,\Gamma_{nr0})$ $\approx 10^{8-9}s^{-1}$. In the presence of a metal nanoparticle cluster, the intense localized optical field of the resonant plasmons increases the population rate of the excited states, acting like a plasmonic pumping source, forcing the electrons to emit from higher vibrational excited states $S_1(\omega\text{-}\,\omega_0)$ to the ground states $S_1(0)$ in which $\omega_0 < \omega < \omega_{ex}$. Thus, the modified decay rate state becomes comparable to the internal relaxation rate: $\Gamma_{int} \leq \Gamma_{r0}+\,\Gamma_{nr0}+\Gamma_{ET}$. The fluorescent nanocrystals are directed to emit at the resonance frequencies of the plasmonic nanostructures, generating new blueshifted fluorescence emission bands, as a result of matching the resonant plasmon modes

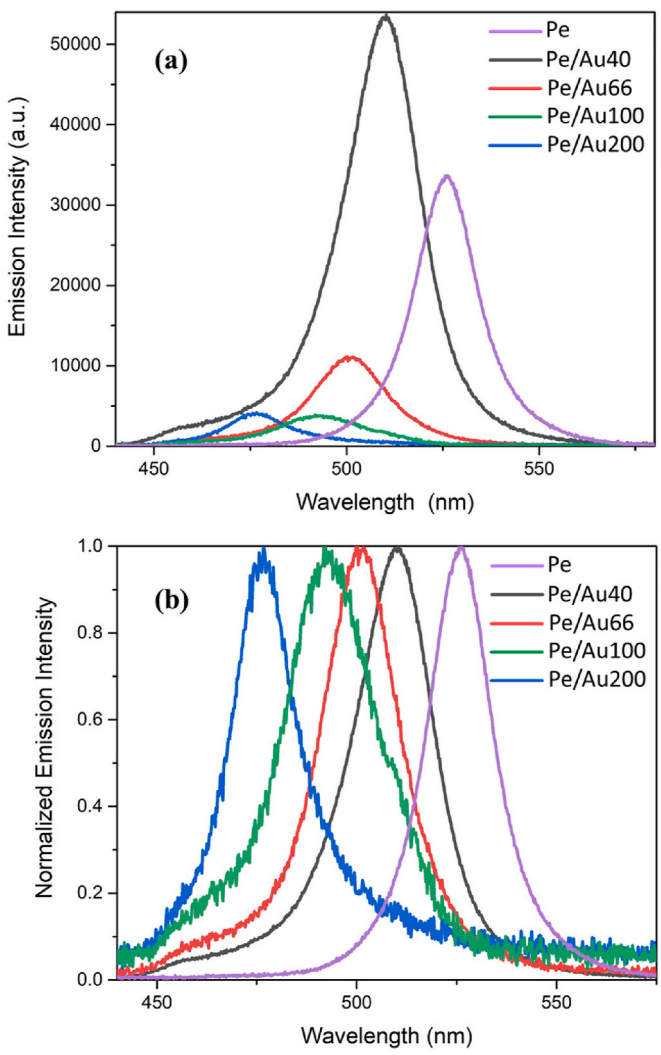


**Fig. 4.** (a) The surface enhanced fluorescence emission spectra and (b) the normalized emission spectra of the neat NWs in polymer medium and the NWs embedded in specific Au nanoparticle clusters in a PS medium.

with the vibrational transitions.

Spectral density of the radiated power, $n_{FDSEF}(\omega_{em})$, is approximately determined by

$$n_{FDSEF}(\omega_{em}) = \frac{|M_{ex}(\lambda ex)|^2}{\eta_0(\omega_{em})}\left[\frac{\gamma_{r0}(\omega_{em}-\omega_{ex}+\omega_0)|M_{em}(\omega_{em},d_{av})|^2}{(\Gamma_{rad}+\Gamma_{ET}+\Gamma_{nr0})}\right]\sigma_{abs}(\omega_{ex})n_L(\omega_{ex}), \quad (1)$$

in which $M_{ex}(\lambda_{ex})$ and $M_{ex}(\omega_{em}, d_{av})$ are the enhancements in the electric field excitation and emission, respectively; $\lambda_{ex}$, $\omega_{em}$, $\omega_{ex}$, and $d_{av}$ represent the excitation wavelength, angular frequency of the emission, angular frequency of the excitation, and the effective distance between the quantum emitter and the metal surface, respectively; $\gamma_{r0}(\omega_{em}$-$\omega_{ex}+\omega_0)$ is the radiative decay rate at the frequency of $\omega_{em}$-$\omega_{ex}+\omega_0$; $\Gamma_{nr0}$ and $\Gamma_{Rad}$ are the ground state nonradiative and total radiative decay rates, respectively; $\Gamma_{ET}$ is the nonradiative transition rate induced by the energy transfer from the excited quantum source to the metal surface; $\eta_0(\omega_{em})$ is the spectral density of quantum efficiency of the fluorescent emitter; $\sigma_{abs}(\omega_{ex})$ is the absorption cross section of the nanocrystal at the angular frequency of excitation; and $n_L(\omega_{ex})$ is the power density of the excitation source. In our study, the enhancement in the electromagnetic field, $M_{ex}(\omega_{em}, d_{av})$ varies from hotspot to hotspot for each Au nanoparticle cluster due to their different plasmon resonances, causing dramatic variations in the surface enhanced fluorescence emission spectra. Thus and so, controlling the emission dynamics of the NWs via a plasmonic modulation is successfully accomplished by introducing the distinctive characteristics of the gold nanostructures in the random media in which the distance between the individual plasmonic nanoparticles and the size distribution of the Au nanoparticle aggregates play a crucial factor [54], arising from different Au nanoparticle concentrations given in Table 1. As demonstrated in the absorption spectrum given in Fig. 1e, the plasmonic characteristics of the Au nanoparticles in a dispersion becomes more distinct and stronger at the wavelength of 520 nm. However, after the plasmonic nanoparticles aggregate in polymeric medium, via increasing the concentration of the plasmonic nanoparticles, strong light absorption is also expected to occur above the wavelength of 520 nm [55,56], which significantly alters the emission dynamics of the interacting NWs. While our measurements confirm that the probability of obtaining clusters of larger sizes from higher Au nanoparticle concentrations is more probable for each sample given in Table 1, the possibility of obtaining larger and more concentrated plasmonic nanoparticle-aggregates, and hence, having a potential of possessing stronger extinction coefficients, dramatically increases from sample 1 to sample 4. Therefore, each nanocluster in a PS film sample may display a unique plasmonic characteristics, leading to a different spectral profile of the interacting quantum source. Hence, in the experiments, the larger plasmonic nanoclusters surrounding the Perovskite NWs are chosen for each sample given in Table 1 to investigate the surface enhanced fluorescence emission spectra, which are presented in Fig. 4.

A 3D finite difference time domain (FDTD) technique is also utilized to verify the strong field enhancement of the dipole interacting with a gold nanoparticle cluster. The perspective and top views of the gold nanoparticle structure, which is used in our numerical calculations, are given in Fig. 6a and b, respectively. In the simulations, the individual gold nanoparticles with a diameter of 14 mm are combined to form a gold nanoparticle cluster and a dipole is placed inside the nanostructure. The gold nanoparticle cluster is embedded in a polymer medium with a refractive index of 1.6. The electric field distribution profile of the dipole, interacting with the gold nanoparticle cluster, obtained from the numerical calculations, is given in Fig. 6c. The simulation results reveal that as the dipole embedded in a gold nanoparticle cluster emits fluorescence, the localized surface plasmons around the gold nanoparticles become available to dramatically strengthen the electric field intensity as demonstrated in Fig. 6c. In our study, the FDSEF mechanism originates when the dipole of the quantum source, emitting at the wavelength of 526 nm, exists at the hot spot region of the plasmonic nanocluster. Our simulation results reveal that since the intense localized optical field of the resonant plasmons significantly increases the population rates of the excited states of the dipole, a high radiative decay rate enhancement of $\geq 10^4$ is obtained through the plasmonic pumping of the quantum source when the dipole is embedded at the deep subwavelength regions between the individual gold nanoparticles of the plasmonic cluster as shown in Fig. 6. Thus, the modified decay rate of the dipole becomes comparable to the internal relaxation rate to induce FDSEF mechanism when the dipole is placed at the strongly enhanced plasmonic field, which is in good agreement with the experimentally obtained results. However, when the distance between the dipole and the gold nanoparticle surface is specified to be larger than 1 nm, the enhancement of the decay rate is determined to considerably decrease to the values of $<10^3$ so that the FDSEF mechanism, which is attributed to be spectral blueshift of the semiconductor NWs surrounded by gold nanoparticles in PS thin films, is proven to exist in our random media provided that the distance between the Perovskite NWs and gold nanoparticles is smaller than 1 nm.

Additionally, the most concentrated sample (Pe/Au200) is also analyzed to elucidate the spectral modulation of quantum sources embedded in different Au nanoparticle aggregates in the same random polymer medium. Fig. 7 displays photoluminescence spectra of the excited NWs interacting with three different strong field regions: hotspot

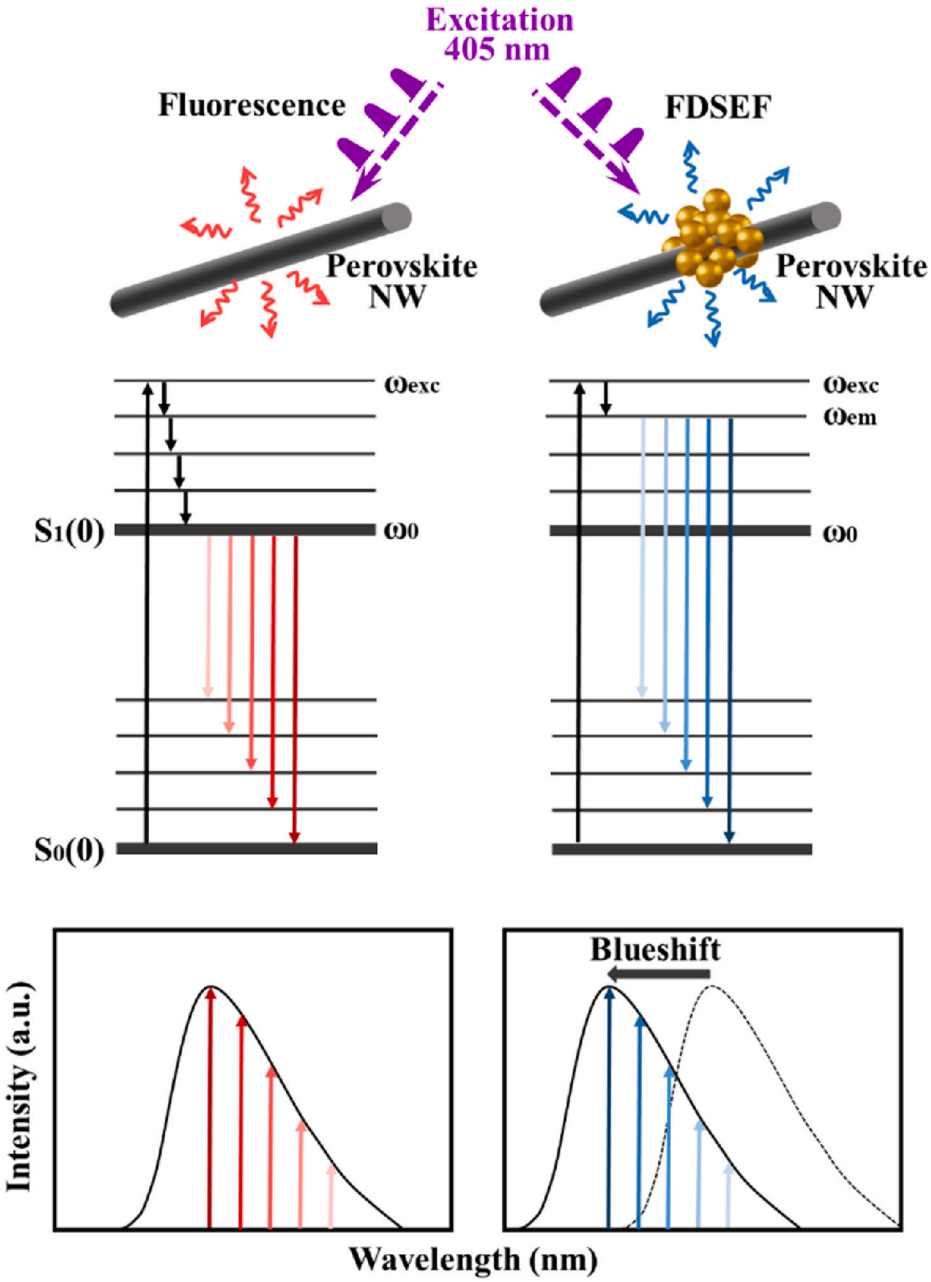


**Fig. 5.** Energy level diagrams and electronic transitions of the Perovskite NWs for fluorescence and FDSEF mechanisms.

(a) 1, (b) 2, and (c) 3; obtained from the sample of Pe/Au200 along with the emission spectrum of the NWs in the absence of plasmonic nanostructure, which confirms that the spectral profile modifications of the semiconductor nanocrystals significantly change from hotspot 1 to 3 in the same polymer medium.

As demonstrated in Fig. 7, the fluorescent nanocrystals in hotspot 1 have a dominant fluorescence emission at the wavelengths of 477.5 nm apart from the fluorescence emission at 502.9 nm. The comparable emission signals at the wavelengths of 455.6 nm and 477.9 nm are also detected from the NWs in the region of hotspot 2. A dominant fluorescence signal at the emission wavelength of 496.7 nm along with the fluorescence emission at 458.5 nm are also observed for the quantum sources in hotspot 3. Therefore, the fluorescence emission spectra of the semiconductor NWs interacting with the hotspot regions display two well-defined emission bands corresponding to the two different plasmon resonance wavelengths in the same hot luminescence region, which may be attributed to be multiple localizations of the electromagnetic fields with distinctive plasmonic characteristics in the same Au nanoparticle aggregates.

In the literature, only a few experimental works on the FDSEF mechanism have been reported [18,25,26], along with some theoretical models to evaluate the plasmon induced-spectral modifications of the interacting dipoles [17]. It is a fact that the strong radiative decay rate enhancement of $>10^3$ is needed to result in a transition for the FDSEF mechanism [24] upon interacting dipoles with the highly concentrated electromagnetic field regions surrounded by plasmonic structures, which is usually obtained by sophisticated nanodevices [57]. For instance, a highly radiative decay rate enhancement of $>10^3$ was revealed using a nanowire device, consisting of CdS–$SiO_2$–Ag core–shell nanostructure, by tuning the size of the plasmonic nanocavity to match with the whispering gallery mode resonance [58]. Nevertheless, a strong plasmonic coupling to the high-energy excited states was also reported via placing the dye molecules on Ag nanoparticle substrates [59], which yields significant spectral modifications of the interacting dipoles.

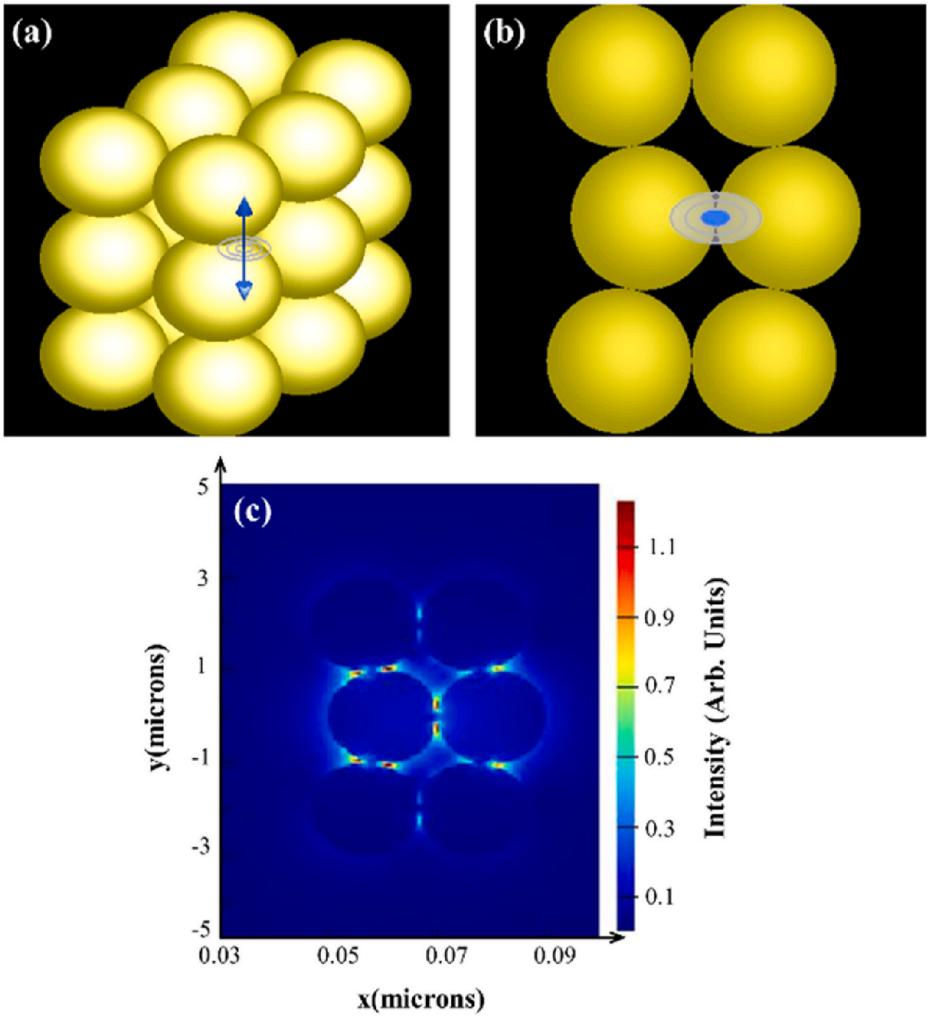


**Fig. 6.** (a) Perspective and (b) top views of a gold nanoparticle cluster used in the simulations. (c) The top view electric field distribution profile of the dipole surrounded by the gold nanoparticle cluster.

Furthermore, the blueshift in the fluorescence emission spectra of the fluorophore molecules induced by the FDSEF mechanism was demonstrated to be controlled using different aspect ratio of the Ag nanowires in random media, similar to our experimental results [27]. The fast and the slow electronic transitions through the enhanced fluorescence emission, which cause spectral distortions of the fluorescence emitters, were even reported using Zn nanoparticle films by Knoblauch et al. [60] although Zn does not provide surface plasmons as much as the metal nanoparticles do. In all these studies, the FDSEF mechanism has been accomplished using fluorophore molecules close to the metal surfaces; nonetheless, in our study, the fluorescence dynamics of the semiconductor Perovskite nanocrystals with their outstanding photovoltaic properties, embedded in Au nanoparticle aggregates, are investigated for the first time to achieve FDSEF mechanism.

Usually tuning emission characteristics of the quantum light emitters through the interaction with the plasmonic nanoparticles is considered to be reversible, which is not the case in our photonic system in concern. Because in this study, stronger or weaker aggregations of the Au nanoparticles surrounding the fluorescent NWs in random polymer media with varying plasmon resonances are formed to alter the FDSEF mechanism. Such control of the plasmonic pumping of the quantum sources at different resonant frequencies allows to obtain the effects of the varied localized surface plasmon characteristics on the spectral modifications of the interacting Perovskite NWs, which means that tuning of the emission dynamics of the fluorescent emitters is ensured by different composition of the nanostructures. As a result, the tunable blueshift in the fluorescence emission spectra of the semiconductor NWs in hotspot regions is achieved for the first time, using different Au nanoparticle aggregates with distinctive plasmonic characteristics.

Additionally, the surface enhanced fluorescence intensity of the interacting quantum sources with these strong electromagnetic field regions, induced by the gold nanoclusters, is also observed to be inhibited and enhanced. The strongest excitation enhancement exists for the NWs in the interparticle hot spot regions that dominates the total photoluminescence emission spectrum. The intensity of the fluorescence emission signal mostly depends on the number of quantum light emitters interacting with the surface plasmons in each hot spot region, which varies for each Au nanoparticle aggregate in our random polymer media. However, the spectral profile modification of the excited emitters induced by the FDSEF mechanism is independent of the number of the quantum sources, accompanying the enhancement or the inhibition of the fluorescence intensity [1,2]. Our experimental results on the basis of plasmonic random media, consisting of fluorescent Perovskite NWs surrounded by Au nanoparticle aggregates in a PS matrix, are promising for the design of highly efficient light-emitting device applications based on semiconductor nanocrystals with remarkable intrinsic properties.

## 4. Conclusions

In this paper, the plasmon resonance frequency-dependent spectral

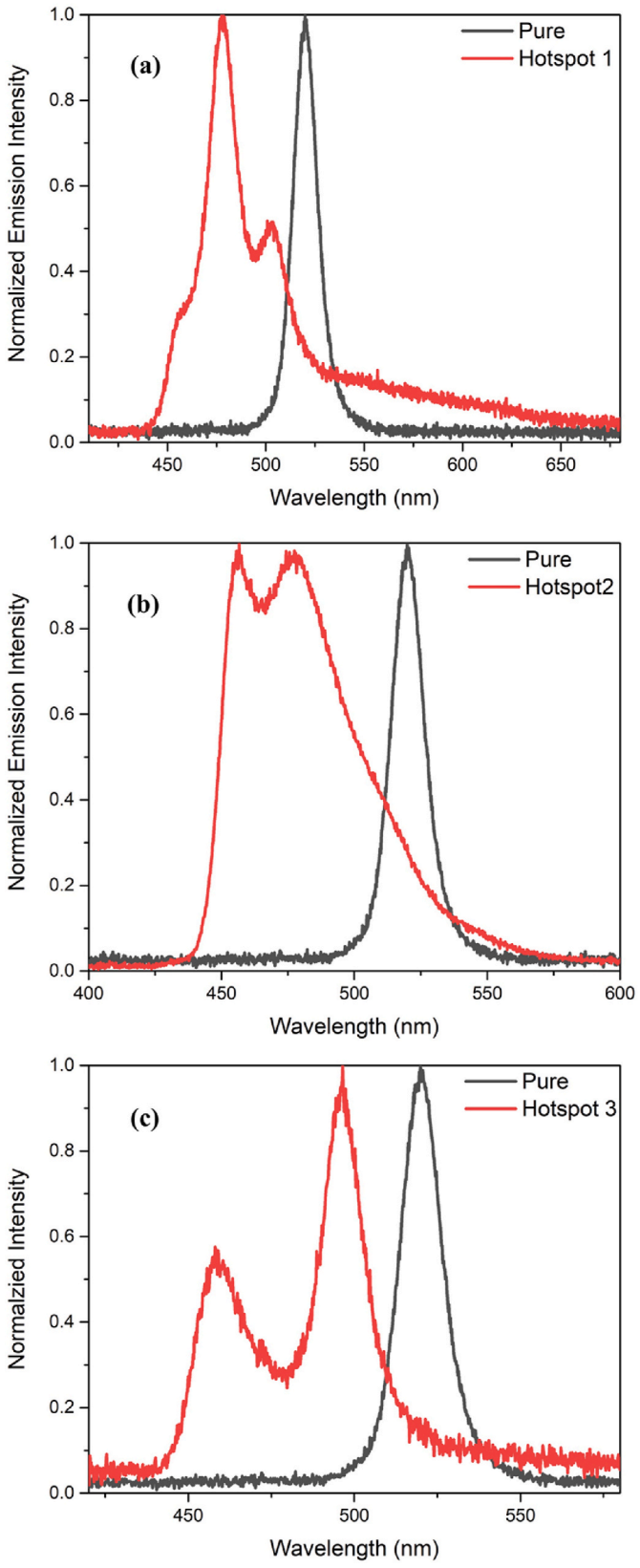


**Fig. 7.** The fluorescence emission spectra of the pure NWs in polymer medium and the NWs interacting with hotspots (a) 1, (b) 2, and (c) 3 in random media of the sample 4 (Pe/Au200).

tunability of the Perovskite NWs is achieved. The NWs are surrounded by Au nanoparticle clusters in random polymer media. The surface plasmons around the Au nanoparticle aggregates act like a tunable optical pumping source to direct the Perovskite NWs into the higher vibrational excited energy state levels, which results in significant variations in the transition rates, causing a blueshift and also some modulation in the spectral profile of the emitters as a result of the dipoles interacting with the strongly localized electromagnetic field regions. The fluorescence intensity signal is also observed to be enhanced and inhibited upon plasmonic pumping of the fluorescent emitters. FDSEF mechanism is attributed to be the tunable-blueshifted fluorescence emission signal of the Perovskite NWs in the hotspot regions. This study has a potential for further investigations of the interactions between the semiconductor nanocrystals and the plasmonic nanoparticles to control the light-matter interaction in various device applications.

## CRediT authorship contribution statement

**Belkıs Gökbulut:** Formal analysis, Writing – original draft, designed and performed the experiments, derived the models, and analyzed the data, wrote the manuscript in consultation with the other authors. **Gokhan Topcu:** performed the synthesis of the random plasmonic media and Perovskite nanowires. **Mustafa M. Demir:** Mentoring for the manuscript. **M. Naci Inci:** Mentoring for the manuscript.

## Declaration of competing interest

The authors declare that they have no known competing financial interests or personal relationships that could have appeared to influence the work reported in this paper.

## Acknowledgements

Dr. Belkıs Gökbulut acknowledges the Boğaziçi University Research Fund for the financial support provided under Contract Number 16761.

## References

[1] V. Kravtsov, S. Berweger, J.M. Atkin, M.B. Raschke, Control of plasmon emission and dynamics at the transition from classical to quantum coupling, Nano Lett. 14 (2014) 5270–5275.
[2] D. Wang, J. Guan, J. Hu, M.R. Bourgeois, T.W. Odom, Manipulating light–matter interactions in plasmonic nanoparticle lattices, Acc. Chem. Res. 52 (2019) 2997–3007.
[3] L.N. Tripathi, O. Iff, S. Betzold, Ł. Dusanowski, M. Emmerling, K. Moon, Y.J. Lee, S. H. Kwon, S. Höfling, C. Schneider, Spontaneous emission enhancement in strain-induced $WSe_2$ monolayer-based quantum light sources on metallic surfaces, ACS Photonics 5 (2018) 1919–1926.
[4] S. Sun, T. Zhang, Q. Liu, L. Ma, Q. Du, H. Duan, Enhanced directional fluorescence emission of randomly oriented emitters via a metal–dielectric hybrid nanoantenna, J. Phys. Chem. C 123 (2019) 21150–21160.
[5] S. Khatua, P.M.R. Paulo, H. Yuan, A. Gupta, P. Zijlstra, M. Orrit, Resonant plasmonic enhancement of single-molecule fluorescence by individual gold nanorods, ACS Nano 8 (2014) 4440–4449.
[6] A.P. Francisco, D. Botequim, D.M.F. Prazeres, V.V. Serra, S.M.B. Costa, C.A.T. Laia, P.M.R. Paulo, Extreme enhancement of single-molecule fluorescence from porphyrins induced by gold nanodimer antennas, J. Phys. Chem. Lett. 10 (2019) 1542–1549.
[7] I. Kaminska, C. Vietz, Á. Cuartero-González, P. Tinnefeld, A.I. Fernández-Domínguez, G.P. Acuna, Strong plasmonic enhancement of single molecule photostability in silver dimer optical antennas, Nanophotonics 7 (2018) 643–649.
[8] A. Camposeo, L. Persano, R. Manco, Y. Wang, P.D. Carro, C. Zhang, Z.Y. Li, D. Pisignano, Y. Xia, Metal-enhanced near-infrared fluorescence by micropatterned gold nanocages, ACS Nano 9 (2015) 10047–10054.
[9] H. Naiki, S. Masuo, S. Machida, A. Itaya, Single-photon emission behavior of isolated CdSe/ZnS quantum dots interacting with the localized surface plasmon resonance of silver nanoparticles, J. Phys. Chem. C 115 (2011) 23299–23304.
[10] S.T. Kochuveedua, D.H. Kim, Surface plasmon resonance mediated photoluminescence properties of nanostructured multicomponent fluorophore systems, Nanoscale 6 (2014) 4966–4984.
[11] S. D'Agostino, F.D. Sala, L.C. Andreani, Dipole-excited surface plasmons in metallic nanoparticles: engineering decay dynamics within the discrete-dipole approximation, Phys. Rev. B 87 (2013) 205413.

[12] S. D'Agostino, F. Alpeggiani, L.C. Andreani, Strong coupling between a dipole emitter and localized plasmons: enhancement by sharp silver tips, Opt Express 21 (2013) 27602–27610.

[13] M. Hensen, T. Heilpern, S.K. Gray, W. Pfeiffer, Strong coupling and entanglement of quantum emitters embedded in a nanoantenna-enhanced plasmonic cavity, ACS Photonics 5 (2018) 240–248.

[14] P. Vasa, C. Lienau, Strong light–matter interaction in quantum emitter/metal hybrid nanostructures, ACS Photonics 5 (2018) 2–23.

[15] A.V. Sorokin, A.A. Zabolotskii, N.V. Pereverzev, S.L. Yefimova, Y.V. Malyukin, A. I. Plekhanov, Plasmon controlled exciton fluorescence of molecular aggregates, J. Phys. Chem. C 118 (2014) 7599–7605.

[16] G. Zengin, M. Wersäll, S. Nilsson, T.J. Antosiewicz, M. Käll, T. Shegai, Realizing strong light-matter interactions between single-nanoparticle plasmons and molecular excitons at ambient conditions, Phys. Rev. Lett. 114 (2015) 157401.

[17] E.C. Le Ru, P.G. Etchegoin, J. Grand, N. Félidj, J. Aubard, G. Lévi, Mechanisms of spectral profile modification in surface-enhanced fluorescence, J. Phys. Chem. C 111 (2007) 16076–16079.

[18] L. Zhao, T. Ming, H. Chen, Y. Lianga, J. Wang, Plasmon-induced modulation of the emission spectra of the fluorescent molecules near gold nanorods, Nanoscale 3 (2011) 3849–3859.

[19] M. Ringler, A. Schwemer, M. Wunderlich, A. Nichtl, K. Kürzinger, T.A. Klar, J. Feldmann, Shaping emission spectra of fluorescent molecules with single plasmonic nanoresonators, Phys. Rev. Lett. 100 (2008) 203002.

[20] E.C. Le Ru, J. Grand, N. Félidj, J. Aubard, G. Lévi, A. Hohenau, J.R. Krenn, E. Blackie, P.G. Etchegion, Spectral Profile Modifications in Metal-Enhanced Fluorescence, John Wiley & Sons, New Jersey, 2010.

[21] F. Tam, G.P. Goodrich, B.R. Johnson, N.J. Halas, Plasmonic enhancement of molecular fluorescence, Nano Lett. 7 (2006) 496–501.

[22] P. Anger, P. Bharadwaj, L. Novotny, Enhancement and quenching of single-molecule fluorescence, Phys. Rev. Lett. 96 (2006) 113002.

[23] E. Dulkeith, A.C. Morteani, T. Niedereichholz, T.A. Klar, J. Feldmann, S.A. Levi, F. C.J.M. van Veggel, D.N. Reinhoudt, M. Moller, D.I. Gittins, Fluorescence quenching of dye molecules near gold nanoparticles: radiative and nonradiative effects, Phys. Rev. Lett. 89 (2002) 203002.

[24] Y.S. Yamamoto, Y. Ozaki, T. Itoh, Recent progress and frontiers in the electromagnetic mechanism of surface-enhanced Raman scattering, J. Photochem. Photobiol., A C 21 (2014) 81–104.

[25] Z.C. Dong, X.L. Zhang, H.Y. Gao, Y. Luo, C. Zhang, L.G. Chen, R. Zhang, X. Tao, Y. Zhang, J.L. Yang, J.G. Hou, Generation of molecular hot electroluminescence by resonant nanocavity plasmons, Nat. Photonics 4 (2010) 50–54.

[26] T. Itoh, Y.S. Yamamoto, H. Tamaru, V. Biju, N. Murase, Y. Ozaki, Excitation laser energy dependence of surface-enhanced fluorescence showing plasmon-induced ultrafast electronic dynamics in dye molecules, Phys. Rev. B 87 (2013) 235408.

[27] J. Bingi, S. Vidhya, A.R. Warrier, C. Vijayan, Plasmonically tunable blue-shifted emission from Coumarin 153 in Ag nanostructure random media: a demonstration of fast dynamic surface-enhanced fluorescence, Plasmonics 9 (2014) 349–355.

[28] X. Li, F. Cao, D. Yu, J. Chen, Z. Sun, Y. Shen, Y. Zhu, L. Wang, Y. Wei, Y. Wu, All inorganic Halide Perovskites nanosystem: synthesis, structural features, optical properties and optoelectronic applications, Small 13 (2017) 1603996.

[29] D. Bi, W. Tress, M.I. Dar, P. Gao, J. Luo, C. Renevier, K. Schenk, A. Abate, F. Giordano, J.P.C. Baena, Efficient luminescent solar cells based on tailored mixed-cation Perovskites, Sci. Adv. 2 (2016), e1501170.

[30] R.E. Beal, D.J. Slotcavage, T. Leijtens, A.R. Bowring, R.A. Belisle, W.H. Nguyen, G. F. Burkhard, E.T. Hoke, M.D. McGehee, Cesium Lead Halide Perovskites with improved stability for tandem solar cells, J. Phys. Chem. Lett. 7 (2016) 746–751.

[31] G. Nedelcu, L. Protesescu, S. Yakunin, M.I. Bodnarchuk, M.J. Grotevent, M. V. Kovalenko, Fast anion-exchange in highly luminescent nanocrystals of cesium lead halide perovskites (CsPbX3, X= Cl, Br, I), Nano Lett. 15 (2015) 5635–5640.

[32] L. Etgar, The merit of Perovskite's dimensionality; can this replace the 3D Halide Perovskite? Energy Environ. Sci. 11 (2018) 234–242.

[33] B.R. Sutherland, E.H. Sargent, Perovskite photonic sources, Nat. Photonics 10 (2016) 295–302.

[34] F. Deschler, M. Price, S. Pathak, L.E. Klintberg, D.D. Jarausch, R. Higler, S. Hüttner, T. Leijtens, S.D. Stranks, H.J. Snaith, High photoluminescence efficiency and optically pumped lasing in solution-processed mixed Halide Perovskite semiconductors, J. Phys. Chem. Lett. 5 (2014) 1421–1426.

[35] Q. Zhang, R. Su, X. Liu, J. Xing, T.C. Sum, Q. Xiong, High-quality whispering-gallery-mode lasing from Cesium Lead Halide Perovskite nanoplatelets, Adv. Funct. Mater. 26 (2016) 6238–6245.

[36] G. Li, F.W.R. Rivarola, N.J. Davis, S. Bai, T.C. Jellicoe, F. la Peña, S. Hou, C. Ducati, F. Gao, R.H. Friend, Highly efficient Perovskite nanocrystal light-emitting diodes enabled by a universal crosslinking method, Adv. Mater. 28 (2016) 3528–3534.

[37] Z.K. Tan, R.S. Moghaddam, M.L. Lai, P. Docampo, R. Higler, F. Deschler, M. Price, A. Sadhanala, L.M. Pazos, D. Credgington, Bright light-emitting diodes based on organometal Halide Perovskite, Nat. Nanotechnol. 9 (2014) 687–692.

[38] J. Mao, H. Lin, F. Ye, M. Qin, J.M. Burkhartsmeyer, H. Zhang, X. Lu, K.S. Wong, W. C. Choy, All-Perovskite emission architecture for white light-emitting diodes, ACS Nano 12 (2018) 10486–10492.

[39] W. Deng, L. Huang, X. Xu, X. Zhang, X. Jin, S.T. Lee, J. Jie, Ultrahigh-responsivity photodetectors from Perovskite nanowire arrays for sequentially tunable spectral measurement, Nano Lett. 17 (2017) 2482–2489.

[40] D. Amgar, A. Stern, D. Rotem, D. Porath, L. Etgar, Tunable length and optical properties of $CsPbX_3$ (x=Cl, Br, I) nanowires with a few unit cells, Nano Lett. 17 (2017) 1007–1013.

[41] B. Akbali, G. Topcu, T. Guner, M. Ozcan, M.M. Demir, H. Sahin, $CsPbBr_3$ perovskites: theoretical and experimental investigation on water-assisted transition from nanowire formation to degradation, Phys. Rev. Mater. 2 (2018), 034601.

[42] Y. Wang, X. Liu, Q. He, G. Chen, D. Xu, X. Chen, W. Zhao, J. Bao, X. Xu, J. Liu, X. Wang, Reversible transformation between $CsPbBr_3$ Perovskite nanowires and nanorods with polarized optoelectronic properties, Adv. Funct. Mater. 31 (2021) 2011251.

[43] Z. Zhong, S. Patskovskyy, P. Bouvrette, J.H.T. Luong, A. Gedanken, The surface chemistry of Au colloids and their interactions with functional amino acids, J. Phys. Chem. B 108 (2004) 4046–4052.

[44] N. Jiang, X. Zhuo, J. Wang, Active plasmonics: principles, structures and applications, Chem. Rev. 118 (2018) 3054–3099.

[45] X. Han, Y. Liu, Y. Yin, Colorimetric stress memory sensor based on disassembly of gold nanoparticle chains, Nano Lett. 14 (2014) 2466–2470.

[46] J. Turkevich, P.C. Stevenson, J.A. Hillier, Study of the nucleation and growth processes in the synthesis of colloidal gold, Discuss. Faraday Soc. 11 (1951) 55–75.

[47] G. Frens, Controlled nucleation for the regulation of the particle size in monodisperse gold suspensions, Nat. Phys. Sci. (Lond.) 241 (1973) 20–22.

[48] G. Absalan, M. Akhond, H. Ershadifar, M.A. Rezaei, Two-approach study for preparing stable colloidal gold nanoparticles in organic solvents by using 1-dodecyl-3 Methylimidazolium Bromide as an efficient capping and phase transfer agent, Colloid. Surface. 486 (2015) 192–202.

[49] K.V. Sarathy, G. Kulkarni, C. Rao, A novel method of preparing thiol-derivatised nanoparticles of gold, platinum and silver forming superstructures, Chem. Commun. 6 (1997) 537–538.

[50] K.S. Mayya, F. Caruso, Phase transfer of surface-modified gold nanoparticles by hydrophobization with alkylamines, Langmuir 19 (2003) 6987–6993.

[51] T.K. Misra, T.S. Chen, C.Y. Liu, Phase transfer of gold nanoparticles from aqueous to organic solution containing resorcinarene, J. Colloid Interface Sci. 297 (2006) 584–588.

[52] M.H. Muhammed, T. Pradeep, Aqueous to organic phase transfer of $Au_{25}$ clusters, J. Cluster Sci. 20 (2009) 365–373.

[53] A. Swarnkar, R. Chulliyil, V.K. Ravi, M. Irfanullah, A. Chowdhury, A. Nag, Colloidal $CsPbBr_3$ perovskite nanocrystals: luminescence beyond traditional quantum dots, Angew. Chem. 127 (2015) 15644–15648.

[54] N. Jiang, X. Zhuo, J. Wang, Active plasmonics: principles, structures, and applications, Chem. Rev. 118 (2018) 3054–3099.

[55] G. Topcu, T. Guner, E. Inci, M.M. Demir, Colorimetric and plasmonic pressure sensors based on polyacrylamide/Au nanoparticles, Sens. Actuator A Phys. 295 (2019) 503–511.

[56] G. Topcu, M.M. Demir, Effect of chain topology on plasmonic properties of pressure sensor films based on poly(acrylamide) and Au nanoparticles, Sens. Actuator A Phys. 295 (2019) 237–243.

[57] K.J. Russell, T.L. Liu, S. Cui, E.L. Hu, Large spontaneous emission enhancement in plasmonic nanocavities, Nat. Photonics 6 (2012) 459–462.

[58] C.H. Cho, C.O. Aspetti, M.E. Turk, J.M. Kikkawa, S.W. Nam, R. Agarwal, Tailoring hot-exciton emission and lifetimes in semiconducting nanowires via whispering-gallery nanocavity plasmons, Nat. Mater. 10 (2011) 669–675.

[59] R. Knoblauch, H.B. Hamo, R. Marks, C.D. Geddes, Spectral distortions in metal-enhanced fluorescence: experimental evidence for ultra-fast and slow transitions, J. Phys. Chem. C 124 (2020) 4723–4737.

[60] R. Knoblauch, H.B. Hamo, R. Marks, C.D. Geddesa, Spectral distortions in Zinc-based metal-enhanced fluorescence underpinned by fast and slow electronic transitions, Chem. Phys. Lett. 744 (2020) 137212.